

Wall-to-wall mapping of peat depth from Lidar terrain and airborne radiometrics in Norwegian landscapes

Julien Vollering¹, Naomi Gatis², Mette Kusk Gillespie¹, Karl-Kristian Muggerud¹, Sigurd Daniel Nerhus¹, Knut Rydgren¹, and Mikko Sparf¹

¹Department of Civil Engineering and Environmental Sciences, Western Norway University of Applied Sciences, Norway

²Department of Geography, University of Exeter, United Kingdom

Correspondence: Julien Vollering (julien.vollering@hvl.no)

Abstract. The abstract goes here. It can also be on *multiple lines*.

1 Introduction

Introduction text goes here. Read Gatis et al. (2019) and related work (Minasny et al., 2019).

2 Materials and methods

5 2.1 Sites

We assessed how well we could predict peat depth at two sites with conspicuously different physical geography: Skrimfjella in eastern Norway and Ørskogfjellet in western Norway (Fig. 1c). These sites were chosen because they were covered by radiometric data from airborne surveys, relatively little built-up area, and road access.

At Skrimfjella we delineated a study area of 34 km² based on radiometric coverage and accessibility (Fig. 1b). The study
10 area has a diverse bedrock, with 32 % alkali feldspar granite, 26 % mergelstein, 10 % granite, and eight other types with > 1 % coverage (NGU, 1:250 000 dataset). The landscape within our delineation is classified as *inland hills and mountains* (Simensen et al., 2021). It is almost without human infrastructure, dominated by forest, and borders on a large nature reserve. The study area has a mean elevation of 438 m above sea level (range 223–711, IQR 351–509), and its mean slope at 10 m resolution is 10.8° (IQR 4.6–15.1°). In Norway’s AR5 national land capability dataset (Ahlstrøm et al., 2019), 1.5 km² (4.5 %) of the study
15 area is classified as mire — defined as areas with mire vegetation and at least 30 cm of peat depth.

At Ørskogfjellet we defined a study area of 124 km² which basically followed the footprint of the radiometric survey (Fig. 1a). According to the Geological Survey of Norway, bedrock in the area is 84 % granitic gneiss, 11 % granite, and 5 % aluminium silicate gneiss (NGU, 1:250 000 dataset). This study area comprises a wide range of major landscape types: *coastal plains*, *coastal fjord*, *inland valleys*, as well as *inland hills and mountains* (Simensen et al., 2021). It is mostly forested, but
20 also contains considerable farmland and open upland, and has several large lakes. Its mean elevation is 211 m above sea level



Figure 1. Study areas at Ørskogfjellet (a) and Skrimfjella (b) within southern Norway (c). Land cover shown here is from the AR50 national land resource database and has simplified geometry with respect to the AR5 database used in the study.

(range 0–807, IQR 73–310), and its mean slope at 10 m resolution is 13.0° (IQR 4.7–18.3°). The AR5 dataset counts 15.3 km² (12.4 %) of the study area as mire.

2.2 Peat depth measurements

At both study sites, our measurements of peat depth were made for the purpose of training a machine learning model of peat depth, and we designed our sampling with this in mind (Brus, 2019). Broadly, we aimed for a sample that was representative the predictor space of the most important predictors of peat depth (Wadoux et al., 2019; Ma et al., 2020). A sample that preserves the properties of the multivariate distribution of predictor and outcome variables is most likely to maintain any complex, non-linear relationships that exist in the population while avoiding spurious ones (Brus, 2019). We chose for our sampling and modelling a spatial resolution of 10 m. We considered this a reasonable compromise between digital terrain model resolution (1 m) and small mires on the one hand, and airborne radiometric resolution (50 m) on the other.

2.2.1 Skrimfjella

We measured peat depth in selected locations (10 m raster cells) at Skrimfjella. The locations were chosen only from areas delineated as mire in the AR5 national land capability dataset. Within this mire area, we stratified our sample across values of elevation, slope, and potassium ground concentration (from processed airborne gamma ray spectrometry, Baranwal et al., 2013). Specifically, we used the *eSample* function in the *iSDM* R package (v.1.0) to chose an environmentally systematic sample. This function defines the environmental space as a two-dimensional convex hull around the ordinated data, then creates a regular grid across that space, and lastly finds for each grid cell the datum that is nearest (Hattab et al., 2017). Elevation was extracted from the 10 m national digital terrain model, slope calculated in degrees, and potassium ground concentration downsampled with bilinear resampling. We set a target sample size of 100, excluded the top and bottom percentile from the convex hull, and with these parameters *eSample* returned 105 raster cells.

In addition to the peat depth locations, we had another arm of our sampling design for measuring peatland occurrence, as binary variable. We wanted to measure peatland occurrence outside of mapped mire areas because the AR5 dataset is known to underestimate peatland coverage (especially in forests, Bryn et al., 2018), and because airborne radiometrics may help identify unmapped peatland (Gatis et al., 2019; O’Leary et al., 2022). The occurrence locations were sampled from the part of the study area that (1) was mapped as something other than mire in the AR5 database and (2) had a slope < 20°. We performed environmentally systematic sampling of this population with the same procedure as for the depth locations, and *eSample* returned 106 raster cells.

Field work at Skrimfjella was conducted in August 2020. We navigated to the centers of the raster cells in the depth and occurrence samples by handheld GPS, checking that positional error was below 3 m. For each depth sample location, we measured peat depth three times (at the vertices of a triangle with 2 m sides) to get a more representative value for the 10 m raster cell, and to dampen the effect of outlying measurements (Parry et al., 2014). We used a metal probe pushed downward until resistance indicated the base of the peat column. Probe locations were adjusted up to 20 cm if the base of the peat column seemed to be blocked by an obvious artifact. For each occurrence sample location, we recorded the presence or absence of

peatland — primarily by digging and examining the top 20 cm of soil (where this was possible). We judged whether the soil
55 was a peat soil based on its density, texture, and color. Occasionally, when the soil itself was difficult to judge, we made our
determination also based on the presence or absence of mire vegetation. Although peat soil is strictly defined by organic content
(which we did not analyse), we believe our protocol produced reasonable determinations of presence or absence that would
generally satisfy most of the varying definitions of peatland (Minasny et al., 2023).

Besides the depth and occurrence measurements described above, we also measured peat depth in three subjectively-chosen,
60 individual mires, using ground-penetrating radar (GPR). We used the Malå ProEx GPR system (Guideline Geo AB, Sweden)
with its 500 MHz shielded antenna mounted in a plastic sledge, and its control unit connected to a GNSS receiver. At each of
the three mires we recorded GPR traces along walking transects that covered the extent of the mire, mostly in traversing, zigzag
patterns with between 5 m and 20 m spacing at their vertices. Along the GPR transects we also probed peat depth at marked
trace locations, to be able to calibrate the GPR wave speed velocity. We processed the GPR data with Reflex2DQuick software
65 (v.3.0; Sandmeier Scientific Software, Germany), applying a time-zero correction, a dewow filter, and a gain filter based on
observed energy decay. Then we picked strong reflectors in the radargrams that we interpreted as the base of the peat column.
We used picks at marked trace locations to calibrate wave speed velocity; we pooled calibration points across the three mires
and fitted a linear regression of depth on one-way travel time with the intercept fixed at zero. In total we had 46 calibration
points along 3.5 km of GPR transects. Finally, we used the calculated wave velocity (0.0387 m ns^{-1} , $R^2 = 0.874$) to convert
70 the travel times of all picks to calibrated peat depths.

2.2.2 Ørskogfjellet

At Ørskogfjellet we also measured peat depth in a sample of 10 m raster cells, selected from the part of the study area classified
in the AR5 dataset as mire. Before selecting locations, we determined a minimal sample size that would adequately capture the
terrain and radiometric properties of the entire mire area. Specifically, we aimed to identify the size at which adding locations
75 produced diminishing decreases in divergence between sample and population distributions — i.e. the elbow point in a curve
of similarity between sample and population (Malone et al., 2019). This approach has been found to identify sample sizes that
correspond with diminishing returns in predictive model performance on external evaluation data (Saurette et al., 2023). We
defined a sequence of increasing sample sizes (50–500) and for ten replicate samples at each size (drawn by conditioned latin
hypercube sampling, Minasny and McBratney, 2006; Roudier, 2011), we calculated the mean Kullback-Leibler divergence
80 between sample and population distributions (Malone et al., 2019; Saurette et al., 2023). The variables in the divergence
calculation were terrain slope and four radiometrics: potassium, thorium, uranium, and total count. Next, we fitted a asymptotic
regression of mean divergence on sample size, and identified the sample size at which the curve reached 95 % of the fitted
asymptote. Through this procedure we found that we could adequately capture the population distribution with a sample of
160 locations.

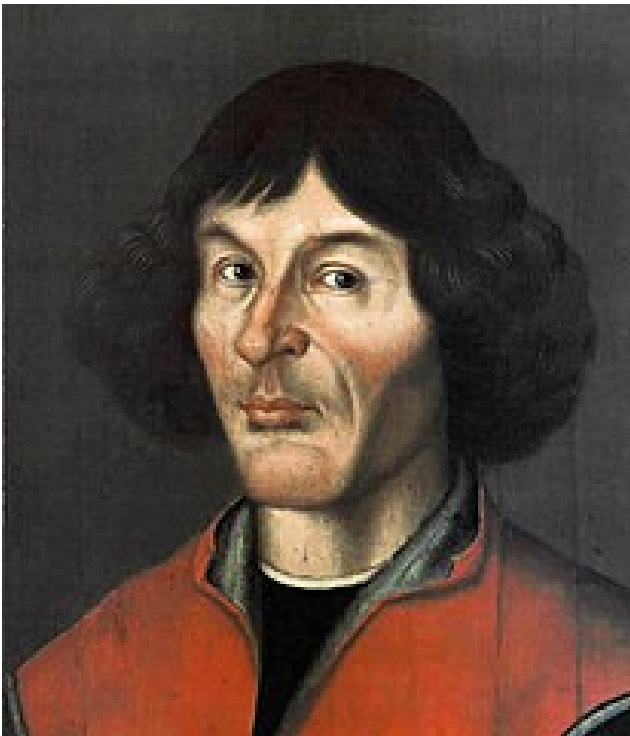


Figure 2. one column figure

Table 1. TEXT

a	b	c
1	2	3

Table Footnotes

85 **2.3 Peat depth predictors**

2.4 Predictive models of peat depth

3 Results

Include a 12cm width figure of Nikolaus Copernicus from Wikipedia with caption using R Markdown (Fig. 2).

3.1 Tables

90 You can add `\LaTeXtable` in an R Markdown document to meet the template requirements (Table 1).

Or you can use markdown to create the table with `booktabs = FALSE` (<https://github.com/rstudio/rarticles/issues/558#issuecomment-19079>)

Table 2. My caption

	mpg	cyl	disp
Mazda RX4	21.0	6	160
Mazda RX4 Wag	21.0	6	160
Datsun 710	22.8	4	108

See Table 2.

4 Discussion

95 Lorem ipsum dolor sit amet, consectetur adipiscing elit. Sed do eiusmod tempor incididunt ut labore et dolore magna aliqua. Ut enim ad minim veniam, quis nostrud exercitation ullamco laboris nisi ut aliquip ex ea commodo consequat. Duis aute irure dolor in reprehenderit in voluptate velit esse cillum dolore eu fugiat nulla pariatur. Excepteur sint occaecat cupidatat non proident, sunt in culpa qui officia deserunt mollit anim id est laborum.

5 Conclusions

100 Nulla facilisi. Maecenas vel nunc nec purus tincidunt congue. Proin auctor, lectus eu pharetra malesuada, nisi nunc bibendum nunc, eget tincidunt nunc nisi id nunc. Sed euismod, nunc sit amet aliquam tincidunt, nunc nunc tincidunt nunc, nec tincidunt nunc nunc nec nunc. Donec auctor, nunc sit amet aliquam tincidunt, nunc nunc tincidunt nunc, nec tincidunt nunc nunc nec nunc.

. *Code and data availability.* Use this to add a statement when having data sets and software code available

Appendix A: For submission

105 “Appendices: all material required to understand the essential aspects of the paper such as experimental methods, data, and interpretation should preferably be included in the main text. Additional figures, tables, as well as technical and theoretical developments which are not critical to support the conclusion of the paper, but which provide extra detail and/or support useful for experts in the field and whose inclusion in the main text would disrupt the flow of descriptions or demonstrations may be presented as appendices. These should be labelled with capital letters: Appendix A, Appendix B etc. Equations, figures and
110 tables should be numbered as (A1), Fig. B5 or Table C6, respectively. Please keep in mind that appendices are part of the manuscript whereas supplements (see below) are published along with the manuscript.”

Appendix B: Figures and tables in appendices

Please also sort the appendix figures and appendix tables into the respective appendix sections. They will be correctly named automatically.

115 Appendix C: Copernicus from Rmarkdown

Please note: Per their guidelines, Copernicus does not support additional \LaTeX packages or new \LaTeX commands than those defined in their `.cls` file. This means that you cannot add any extra dependencies and a warning will be thrown if so. **Important:** Always double-check with the official manuscript preparation guidelines at https://publications.copernicus.org/for_authors/manuscript_preparation.html, especially the sections “Technical instructions for LaTeX” and “Manuscript
120 composition”. Please contact Daniel Nüst, `daniel.nuest@uni-muenster.de`, with any problems.

. *Author contributions.* JV: Conceptualization, Investigation, Data curation, Formal analysis, Writing – original draft. NG: Conceptualization, Methodology, Writing - review & editing. MKG: Investigation, Writing - review & editing. KKM: Investigation, Data curation, Writing - review & editing. SDN: Investigation, Writing - review & editing. KR: Conceptualization, Investigation, Writing - review & editing. MS: Investigation, Data curation, Writing - review & editing.

125 . *Competing interests.* The authors declare that they have no conflict of interest.

. *Disclaimer.* The authors declare that the results, discussions, and interpretations presented in this study are solely their own. The views expressed herein do not necessarily reflect those of their respective institutions or funding agencies.

. *Acknowledgements.* We thank the Norwegian Public Roads Administration for sharing data from ground-penetrating radar surveys. We also thank Vikas Baranwal from the Geological Survey of Norway for helping us access the radiometric data from Skrim. This work contains
130 data under the following licenses: (1) Creative Commons Attribution 4.0 International, © Kartverket, (2) *Norge digitalt* license, Norwegian Institute of Bioeconomy Research (NIBIO), © Geovekst, and (3) the Norwegian License for Public Data (NLOD), made available by the Geological Survey of Norway (NGU).

References

- Ahlstrøm, A., Bjørkelo, K., and Fadnes, K. D.: AR5 Klassifikasjonssystem, Tech. rep., NIBIO, 2019.
- 135 Baranwal, V., Rodionov, A., Ofstad, F., Koziel, J., and Lynum, R.: Helicopter-Borne Magnetic, Electromagnetic and Radiometric Geophysical Surveys in the Kongsberg Region: Krøderen, Sokna, Hønefoss, Kongsberg and Numedalen., Tech. Rep. 2013.029, Geological Survey of Norway, 2013.
- Brus, D. J.: Sampling for Digital Soil Mapping: A Tutorial Supported by R Scripts, *Geoderma*, 338, 464–480, <https://doi.org/10.1016/j.geoderma.2018.07.036>, 2019.
- 140 Bryn, A., Strand, G.-H., Angeloff, M., and Rekdal, Y.: Land Cover in Norway Based on an Area Frame Survey of Vegetation Types, *Norwegian Journal of Geography*, 72, 131–145, <https://doi.org/10.1080/00291951.2018.1468356>, 2018.
- Gatis, N., Luscombe, D., Carless, D., Parry, L., Fyfe, R., Harrod, T., Brazier, R., and Anderson, K.: Mapping Upland Peat Depth Using Airborne Radiometric and Lidar Survey Data, *Geoderma*, 335, 78–87, <https://doi.org/10.1016/j.geoderma.2018.07.041>, 2019.
- Hattab, T., Garzón-López, C. X., Ewald, M., Skowronek, S., Aerts, R., Horen, H., Brasseur, B., Gallet-Moron, E., Spicher, F., Decocq, G.,
145 Feilhauer, H., Honnay, O., Kempeneers, P., Schmidtlein, S., Somers, B., Kerchove, R. V. D., Rocchini, D., and Lenoir, J.: A Unified Framework to Model the Potential and Realized Distributions of Invasive Species within the Invaded Range, *Diversity and Distributions*, 23, 806–819, <https://doi.org/10.1111/ddi.12566>, 2017.
- Ma, T., Brus, D. J., Zhu, A.-X., Zhang, L., and Scholten, T.: Comparison of Conditioned Latin Hypercube and Feature Space Coverage Sampling for Predicting Soil Classes Using Simulation from Soil Maps, *Geoderma*, 370, 114–136, <https://doi.org/10.1016/j.geoderma.2020.114366>, 2020.
150
- Malone, B. P., Minansy, B., and Brungard, C.: Some Methods to Improve the Utility of Conditioned Latin Hypercube Sampling, *PeerJ*, 7, e6451, <https://doi.org/10.7717/peerj.6451>, 2019.
- Minasny, B. and McBratney, A. B.: A Conditioned Latin Hypercube Method for Sampling in the Presence of Ancillary Information, *Computers & Geosciences*, 32, 1378–1388, <https://doi.org/10.1016/j.cageo.2005.12.009>, 2006.
- 155 Minasny, B., Berglund, Ö., Connolly, J., Hedley, C., de Vries, F., Gimona, A., Kempen, B., Kidd, D., Lilja, H., Malone, B., McBratney, A., Roudier, P., O’Rourke, S., Rudiyanto, Padarian, J., Poggio, L., ten Caten, A., Thompson, D., Tuve, C., and Widyatmanti, W.: Digital Mapping of Peatlands – A Critical Review, *Earth-Science Reviews*, 196, 102–170, <https://doi.org/10.1016/j.earscirev.2019.05.014>, 2019.
- Minasny, B., Adetsu, D. V., Aitkenhead, M., Artz, R. R. E., Baggaley, N., Barthelmes, A., Beucher, A., Caron, J., Conchedda, G., Connolly, J., Deragon, R., Evans, C., Fadnes, K., Fiantis, D., Gagkas, Z., Gilet, L., Gimona, A., Glatzel, S., Greve, M. H., Habib, W.,
160 Hergoualc’h, K., Hermansen, C., Kidd, D. B., Koganti, T., Kopansky, D., Large, D. J., Larmola, T., Lilly, A., Liu, H., Marcus, M., Middleton, M., Morrison, K., Petersen, R. J., Quaife, T., Rochefort, L., Rudiyanto, Toca, L., Tubiello, F. N., Weber, P. L., Weldon, S., Widyatmanti, W., Williamson, J., and Zak, D.: Mapping and Monitoring Peatland Conditions from Global to Field Scale, *Biogeochemistry*, <https://doi.org/10.1007/s10533-023-01084-1>, 2023.
- O’Leary, D., Brown, C., and Daly, E.: Digital Soil Mapping of Peatland Using Airborne Radiometric Data and Supervised Machine Learning – Implication for the Assessment of Carbon Stock, *Geoderma*, 428, 116–136, <https://doi.org/10.1016/j.geoderma.2022.116086>, 2022.
- 165 Parry, L., West, L., Holden, J., and Chapman, P.: Evaluating Approaches for Estimating Peat Depth, *Journal of Geophysical Research: Biogeosciences*, 119, 567–576, <https://doi.org/10.1002/2013JG002411>, 2014.
- Roudier, P.: Clhs: A R Package for Conditioned Latin Hypercube Sampling., 2011.

- 170 Saurette, D. D., Heck, R. J., Gillespie, A. W., Berg, A. A., and Biswas, A.: Divergence Metrics for Determining Optimal Training Sample Size in Digital Soil Mapping, *Geoderma*, 436, 116 553, <https://doi.org/10.1016/j.geoderma.2023.116553>, 2023.
- Simensen, T., Erikstad, L., and Halvorsen, R.: Diversity and Distribution of Landscape Types in Norway, *Norsk Geografisk Tidsskrift - Norwegian Journal of Geography*, 75, 79–100, <https://doi.org/10.1080/00291951.2021.1892177>, 2021.
- Wadoux, A. M. J.-C., Brus, D. J., and Heuvelink, G. B. M.: Sampling Design Optimization for Soil Mapping with Random Forest, *Geoderma*, 355, 113 913, <https://doi.org/10.1016/j.geoderma.2019.113913>, 2019.